

## Measurement of single leukemia cell's density and mass using optically induced electric field in a microfluidics chip

Yuliang Zhao,<sup>1</sup> Hok Sum Sam Lai,<sup>1</sup> Guanglie Zhang,<sup>1,a)</sup> Gwo-Bin Lee,<sup>2</sup> and Wen Jung Li<sup>1,b)</sup>

<sup>1</sup>*Department of Mechanical and Biomedical Engineering, City University of Hong Kong, Kowloon, Hong Kong*

<sup>2</sup>*Department of Power Mechanical Engineering, National Tsing Hua University, Hsinchu, Taiwan*

(Received 29 January 2015; accepted 30 March 2015; published online 17 April 2015)

We present a method capable of rapidly ( $\sim 20$  s) determining the density and mass of a single leukemic cell using an *optically induced electrokinetics* (OEK) platform. Our team had reported recently on a technique that combines sedimentation theory, computer vision, and micro particle manipulation techniques on an OEK microfluidic platform to determine the mass and density of micron-scale entities in a fluidic medium; the mass and density of yeast cells were accurately determined in that prior work. In the work reported in this paper, we further refined the technique by performing significantly more experiments to determine a universal correction factor to Stokes' equation in expressing the drag force on a microparticle as it falls towards an infinite plane. Specifically, a theoretical model for micron-sized spheres settling towards an infinite plane in a microfluidic environment is presented, and which was validated experimentally using five different sizes of micro polystyrene beads. The same sedimentation process was applied to two kinds of leukemic cancer cells with similar sizes in an OEK platform, and their density and mass were determined accordingly. Our tests on mouse lymphocytic leukemia cells (L1210) and human leukemic cells (HL-60) have verified the practical viability of this method. Potentially, this new method provides a new way of measuring the volume, density, and mass of a single cell in an accurate, selective, and repeatable manner. © 2015 AIP Publishing LLC. [<http://dx.doi.org/10.1063/1.4917290>]

### I. INTRODUCTION

Just like the weight of a person, the mass of a single cell varies with its experience such as different growth phase and different health status.<sup>1</sup> However, the measurement of single cellular mass and density has proven to be very difficult for biological researchers. The main reason is that the mass of a micron-size cell is very small—about hundreds of picograms—which makes the determination of cell mass very difficult, especially in a fluidic environment.

Bio-microfluidics chips have become essential tools for cell-based assays and observation of cellular behavior,<sup>2</sup> and recently three kinds of methods have been demonstrated to measure a single cell's density and mass. Two well-known methods, i.e., *suspended microchannel resonator* (SMR)<sup>3–5</sup> and *pedestal resonant sensor* (PRS),<sup>6–8</sup> have been developed based on physical approaches using micro resonators. Although both of them involve complicated fabrication and indirect mappings between the cell mass and the measured physics-parameters, these two methods have been found to be applicable in the measurement of the density and mass of single cells.

The *density gradient centrifugation*<sup>9</sup> method is a widely accepted method of measuring the average density of a cell population. After centrifugation, microparticles with different densities

<sup>a)</sup>For computer vision and image processing, correspondence should be addressed to: [gl.zhang@cityu.edu.hk](mailto:gl.zhang@cityu.edu.hk)

<sup>b)</sup>For hydrodynamics and bio-electrokinetics, correspondence should be addressed to: [wenjli@cityu.edu.hk](mailto:wenjli@cityu.edu.hk)

settle in a fluid and are localized at different heights in the fluid contained in a tube. Although the method cannot provide the mass and density values of a single cell, it has provided the insight that if a single cell is allowed to fall freely in a solution, one can calculate the density and mass of a single cell by monitoring its falling velocity and trajectory. Combining this simple “sedimentation” principle with *optically induced electrokinetics* (OEK)<sup>10</sup> technology, we will show in this paper a novel method for single cell density and mass measurement. OEK, essentially a dielectrophoresis (DEP) system, uses digitally and optically projected images to define virtual electrodes instead of metal electrodes. Transport,<sup>11</sup> separation,<sup>12,13</sup> rotation,<sup>14,15</sup> and patterning<sup>16</sup> of micro/nanoparticles, including cells and DNAs, are major features of OEK technology. We have recently developed an OEK-based method capable of measuring the mass and density of a single bead and yeast cell.<sup>17</sup> In that work, a modified equation was derived to describe the correction factor associated with the Stokes’ force acting on a micro-sized polystyrene sphere in deionized (DI) water settling towards the bottom substrate of a microfluidics chamber. The density and mass of the individual yeast cells could then be determined by calculating the settling velocity of a single yeast cell using a modified equation.

However, there are two problems that need to be solved before the aforementioned method could be used for measuring the mass of a single cancer cell. The first arises from the fact that the geometry and electrical properties of yeast and mammalian cells are very different. In DI water, yeast cells under the influence of DEP force and could stay alive for more than 2 h; for the two kinds of cancer cells discussed in this paper, i.e., human leukemic cells (HL-60) and mouse lymphocytic leukemia cells (L1210), lysis could occur easily under the influence of DEP force. Hence, various fluidic media were explored to enable the measurement of the mass of a single mammalian cell in an OEK chip. The second problem of our previous work is that the polystyrene micro beads have been tested using only one kind of fluid, i.e., DI water. The classical method of investigating hydrodynamic interactions involves observing the motion of a sphere as it settles in a viscous oil<sup>18</sup> or a magnetic filed.<sup>19</sup> Therefore, since the viscosity and density of a fluidic medium may also be important factors governing the hydrodynamic interactions associated with a sphere as it approaches a plane within a viscous solution, a generalized equation is required to describe how a particle settles in fluidic media with different viscosity and density values.

We will present here for the first time an OEK-based technique capable of measuring the mass and density of single cancer cells. A rapid, simple, and repeatable method is presented along with the validation of the correction factor related to an equation used to model the Stokes’ force acting on a micro-sized sphere settling towards an infinite plane. Two new fluidic media, i.e., 0.1M and 0.2M sucrose solution, were also tested in an OEK chip in order to obtain a more generalized model for micro particles “sedimenting” in the chip. In this paper, the theoretical model of spheres settling towards an infinite plane in a fluidic environment is presented first. Next, to validate the theory, standard polystyrene beads with diameters from 5  $\mu\text{m}$  to 25  $\mu\text{m}$  were tested experimentally using an OEK system. An image matching algorithm based on a sedimentation video captured on an OEK platform is introduced to facilitate the calculation of the trajectories and velocities of the beads. After the sedimentation velocity is calculated, the new correction factor for Stokes’ force in the new sucrose solutions is validated again. Next, the same sedimentation processing is used for the two kinds of cancer cells with similar diameters (8–15  $\mu\text{m}$ ) to determine the density and mass values of individual cancer cells. We will show that the preliminary results on Mouse lymphocytic leukemia cells (L1210) matched the results measured by SMR well, which verifies the practical viability of our method. Finally, the measured data using the OEK platform for the density and mass values of the HL-60 are also presented.

## II. MATERIALS AND METHODS

### A. Model and theory

For nearly a century, an attractive theoretical problem in viscous fluids has been to understand the long range of hydrodynamic interactions among spherical particles settling towards an infinite plane.<sup>20</sup> This problem has been studied by many researchers under a variety of

conditions: varying Reynold's number values, different settling distances, and different kinds of planes and viscosity solutions, but few have focused their studies in microfluidics environment. When a spherical particle with a diameter  $D \sim 10 \mu\text{m}$  immersed in aqueous solution (viscosity  $\eta \sim 1 \text{ mPa}\cdot\text{s}$  and density  $\rho \sim 10^3 \text{ kg/m}^{-3}$ ) moves at the speed of  $u = 0.5 \mu\text{m/s}$ , the Reynolds number<sup>21</sup> of the flow will be  $Re \sim 10^{-6} \ll 1$ . Reynolds number is defined as  $Re = ur/\eta$ , where  $r$ , the characteristic length scale, can be the radius of the sphere. The number represents the ratio of inertial forces to viscous forces, and a small  $Re$  means that the inertial forces can be neglected compared to the viscous forces. When this sphere is falling perpendicular towards a single, infinite, and plane surface, the classical equation for the particle velocity can be simplified as

$$u = \frac{2r^2 g (\rho_{\text{sphere}} - \rho_{\text{solution}})}{9\eta K}, \quad (1)$$

where  $g$  is the gravitational constant,  $\rho_{\text{sphere}}$  is the density of the particle,  $\rho_{\text{solution}}$  is the density of the solution and  $K$  is the correction factor associated with Stokes' law. From this equation, we can easily conclude that, if the settling velocity and the correction factor are known, the density of the sphere can be calculated.

Fig. 1 shows the main forces acting on a spherical particle during its sedimentation in a solution towards a solid plane. While hydrodynamic interactions among the sphere, solution, and the plane due to the blocking effect of the plane become very complicated, the correction factor  $K$  for the viscosity force has been shown to be very important in determining the motion of the particle in the fluid as the particle approaches a stationary infinite plane. Although a classical hydrodynamics equation of the correction factor for Stokes force has been given by Maude<sup>22</sup> and Brenner<sup>23</sup> fifty years ago (see Eq. (2)), the bipolar-coordinate system of it detracts from being used directly in our situation

$$K = \frac{4}{3} \sinh \alpha \sum_{n=1}^{\infty} \frac{n(n+1)}{(2n-1)(2n+3)} \left[ \frac{2 \sinh(2n+1)\alpha + (2n+1) \sinh 2\alpha}{4 \sinh^2(n+\frac{1}{2})\alpha - (2n+1)^2 \sinh^2 \alpha} - 1 \right], \quad (2)$$

where

$$\cosh \alpha = h/r$$

and  $h$  is the distance between the bottom of the sphere to the plane. When  $h \ll r$ , the theory of lubrication<sup>23</sup> of correct factor  $K$ , also known as Taylor's model, can be expressed as

$$K = \frac{r}{h}. \quad (3)$$

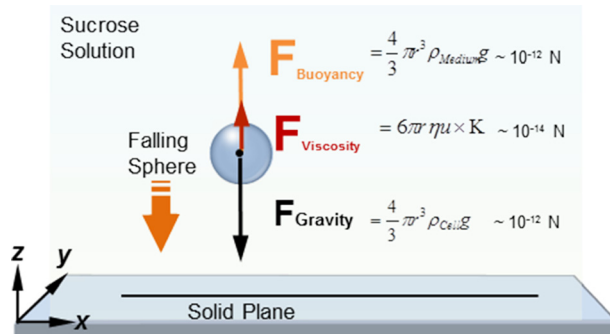


FIG. 1. Illustration showing the forces a sphere encounters during its sedimentation towards a solid plane in the sucrose solution. For a sphere with a diameter of  $10 \mu\text{m}$  and a density of  $\sim 1.05 \text{ g/cm}^3$  settling in a  $0.2\text{M}$  sucrose solution, the magnitudes of the forces are estimated, as shown in the figure.

Most of the classical hydrodynamic models were built macro-environment conditions, so their results may not be suitable for transfer directly to the microfluidics environment. Therefore, classical hydrodynamic models should be validated in micron-sized environments first before actually using them to explain hydrodynamic interactions of biological cells in microfluidic chips. Our previous work<sup>17</sup> had presented a calibration method for two kinds of polystyrene beads (radii equaling  $10.42\ \mu\text{m}$  and  $5.26\ \mu\text{m}$ ) in DI water. The present paper extends that work by presenting experimental data on five kinds of standard polystyrene beads with different diameters ( $5\ \mu\text{m}$ – $25\ \mu\text{m}$ ) settling in three kinds of solutions. We note here that the diameters of the two kinds of cancer cells investigated in this present work are in the range of  $8$ – $15\ \mu\text{m}$ .

As the cell radius is already very small, the precise settling velocity data cannot be obtained within the falling distance range of  $h \ll r$  due to the resolution of the camera. Instead, the experiments were carried out in a falling distance range of  $h < 2r$ , which does not satisfy the assumption behind Eq. (3). For these reasons and because, to the best of our knowledge, there is no other theory suitable for this situation, we fitted the experimental data gathered using standard beads to  $K = ar/h$ , where “ $a$ ” is a dimensionless coefficient. After several hundred times of fitting experiments, “ $a$ ” was found to be a constant. Consequently, the variation in the falling height of the sphere with time could be calculated as

$$h = h_0 e^{-\frac{U_0}{ar}t}, \quad (4)$$

where  $h_0$  is a height factor, decided by the initial falling position, and  $U_0$  is the Stokes velocity<sup>24</sup> of sedimentation in an unbounded fluid. After fitting experimental data related to spheres with known density values to the height-time function,  $h = h_0 e^{-\sigma t}$ , the magnitude of constant  $a$  could be determined from the fitted result of time constant  $\sigma$  in equation  $a = U_0/(\sigma r)$ . Finally, the density of a cell could be written as

$$\rho_{\text{Cell}} = \frac{9\eta a \sigma}{2rg} + \rho_{\text{Medium}}. \quad (5)$$

## B. OEK system

Before letting a single cell fall down freely in a solution medium, the cell needs to be lifted up to a certain height first using optically induced DEP force as discussed earlier. Furthermore, the cells should be in a sucrose solution or a similar culture medium, where the cells can stay alive for a long time and simultaneously allowing the OEK platform to generate sufficient DEP to lift the cells. Fig. 2(a) illustrates the OEK system's configuration. The key part is the OEK chip consisting of a sandwich structure (see Fig. 2(b)), i.e., a photoconductive layer made up of hydrogenated amorphous silicon is deposited on an indium tin oxide coated glass substrate. When a digital image is projected onto the photoconductive layer, the electrical conductivity on the illuminated area is increased locally. This leads to virtual electrodes being formed on the illuminated area. Just as with a metal electrode, a non-uniform electric field is induced which results in a DEP force; this force enables manipulation of microparticles. One can then easily induce the vertical motion of a cell just by turning on or shutting down the light. Whenever the light beam is projected onto the OEK chip, the particle is lifted up and it starts to sediment when there is no light projected. Note that in order to assure that the images are taken with the same illumination; the DEP force can be produced or eliminated, instead, by turning on or shutting off the current applied between the ITO glasses of the chip. Figs. 3(a1), 3(a3), 3(b1), and 3(c1) show the microscopy images of the standard microbeads, L1210, and HL-60 cells, respectively, when there was no DEP force and the cells were in their respective initial states. Figs. 3(a2), 3(b2), 3(c2), and 3(c3) show the images obtained when the current was shut down and the cells were settling down.

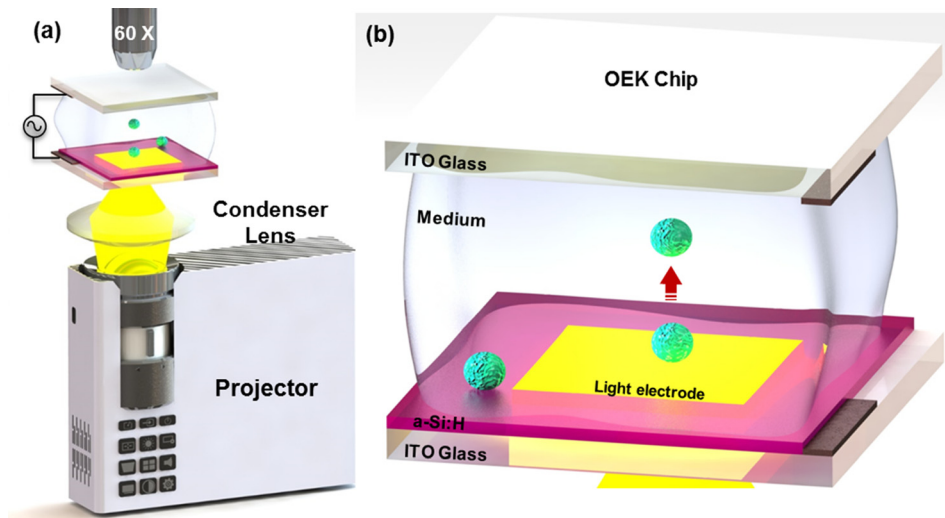


FIG. 2. Illustration showing the manipulation of cell in (a) the OEK system by a digital electric field produced in (b) an OEK chip.

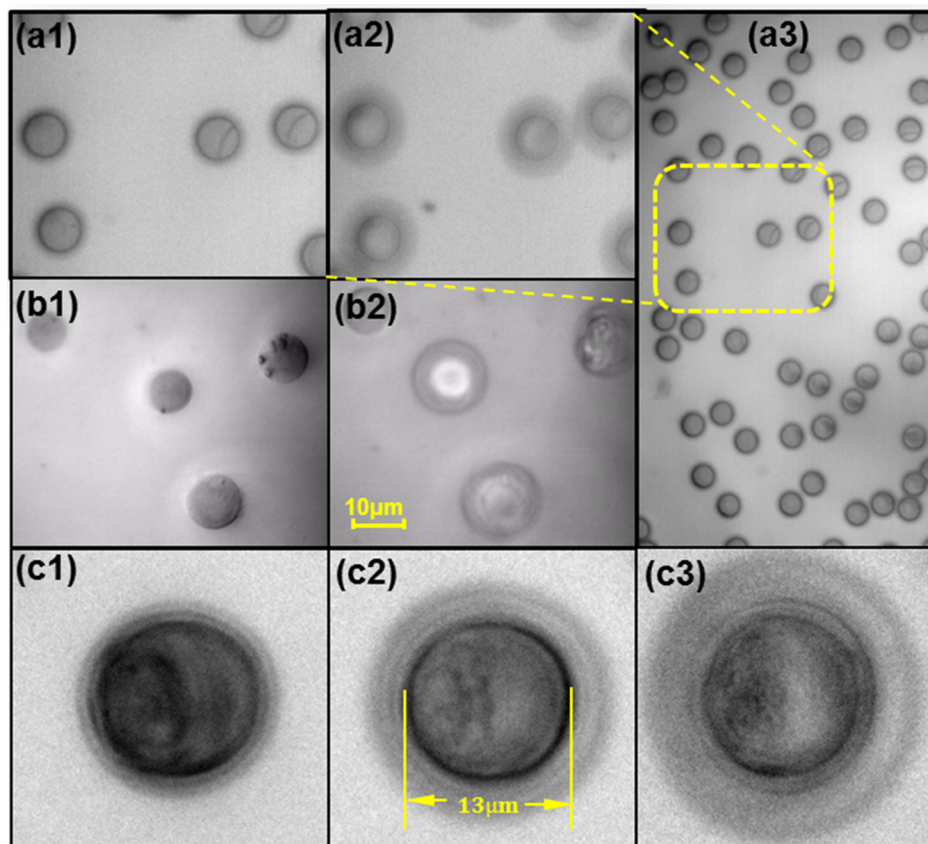


FIG. 3. Microscope pictures of the focusing and defocusing images of (a) micro spheres with a diameter of  $10\mu\text{m}$ , (b) L1210 cells, and (c) HL-60 cells. (a1) and (a2) are the enlarged image of (a3) and (a2) is the relative defocusing image of (a1). (b1) and (c1) are the focusing images of L1210 cells and HL-60 cell in the initial state. The defocusing images of the same HL-60 cell in a falling state were captured when it was (c2)  $5\mu\text{m}$  and (c3)  $10\mu\text{m}$  away from the substrate.



### C. Trajectory tracking and velocity measurement

The micro polystyrene beads were tested first to eventually enable the calculation of cell trajectory and velocity inside the OEK chip. Standard micro beads with radius of  $5\ \mu\text{m}$  were lifted up using the DEP force produced by the OEK chip as described in Sec. II B. After raising them to a certain height (a distance approximately equal to their diameters above the substrate's surface), the DEP force was removed and then the beads were allowed to sediment freely. In our OEK platform, a monocular microscope (NIKON, Ti-E) with a single camera (NIKON, DS-Qi1Mc-U3) was fitted on the top of the OEK chip to record the sedimentation of the spheres. The microscopy system used a CFI Super Plan Fluor lens (ELWD,  $60\times$ , N.A. 0.70, and W.D. 2.61–1.79 mm) with a field-of-view ( $1280 \times 1024$  pixels) which was sufficient to accommodate about 30 cancer cells. A halogen lamp (12 V–100 W LL) was used as the illumination source while capturing the video.

It is very difficult to determine the vertical velocity of a moving bead or cell from a top view just by using a single monocular microscope. However, we solved this problem by using an image matching method that could accurately track the vertical trajectories of the spheres. When the microscope's focal distance was fixed, the defocused images of a sphere at different heights appeared differently, as shown in the image sequence shown on the left side of Fig. 4. Because the diffractive light paths change the images depending on the sphere's distance from the microscope lens, the standard defocused images were captured at different heights first. The location where a particle has the mostly clear image, i.e., a focused image, was set as the “zero height point” and the image (see the left-bottom image in Fig. 4) obtained at this height was selected as the “zero height image.” Next, we let the microscope move its z-axis stage automatically towards the objective lens in  $0.1\ \mu\text{m}$  incremental steps while the microscope captured at each step an image of the static sphere. Once the falling spheres had been captured in a video, the vertical position of each frame could be obtained by comparing them to these standard images. The matching algorithm was based on the image processing technique adopted in our prior work.<sup>17</sup> Both the standard images and the experimental images had to go through noise reduction, sphere recognition, and feature extraction. Following feature correlation comparison between the standard and experimental images, it was straight forward to identify the most similar standard image with known height. Combining the elapsed time information recorded in the video, a distance-time plot was obtained from the sedimentation motion of a

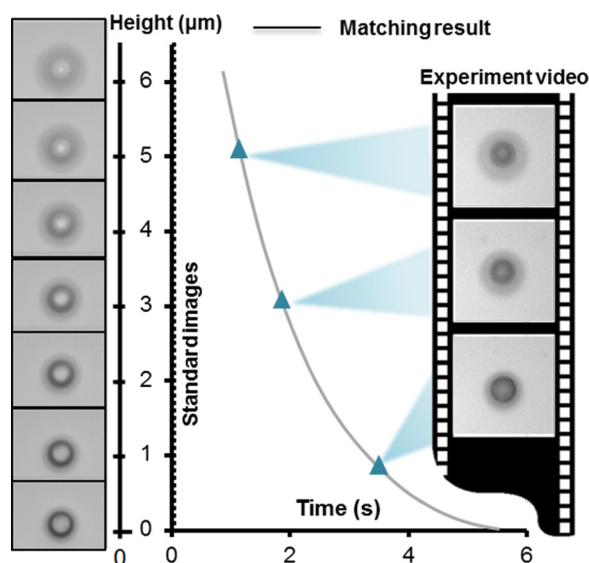


FIG. 4. The matching process of the standard images with the experiment images captured during the sedimentation of a particle.

bead/cell from which the trajectory and velocity of a micro particle during the sedimentation process could be calculated easily.

#### D. Sample preparation

Standard polystyrene microparticles with diameters of 5, 10, 15, 20, and 25  $\mu\text{m}$  (std dev  $< 0.2 \mu\text{m}$  and coeff var  $< 2\%$ ) were obtained from Sigma-Aldrich company. Before each experiment, 3  $\mu\text{l}$  of the particles in aqueous suspension was diluted in a 1.5 ml sucrose solution with a concentration of 0.1M or 0.2M.

L1210 were purchased from American type culture collection (ATCC<sup>®</sup> CCL-219<sup>TM</sup>). L1210 lymphoma cells were grown at 37°C in Liebovitz's L15 medium with glutamine (Gibco, 21083027), 10% (vol/vol) fetal bovine serum (FBS, Gibco, 10438026), 1% 100 $\times$  penicillin-streptomycin (Gibco, 15140-122), and 0.4% (w/vol) glucose (Sigma-Aldrich; G8270).

HL-60 cells were obtained from American type culture collection (ATCC<sup>®</sup> CCL-240<sup>TM</sup>) and cultured at 37°C in the base medium RPMI-1640 (ATCC<sup>®</sup> 30-2001<sup>TM</sup>) with fetal bovine serum to a final concentration of 20%.

Both types of cells were seeded at densities equaling about  $5 \times 10^4$  cells/ml in a 25 cm<sup>2</sup> flask (LabServ, 31010903) in a 5% CO<sub>2</sub> incubator (Model Heracell<sup>®</sup> 150i, Thermo Scientific). The media were refreshed every 2–3 day period after having reached a density of  $1 \times 10^6$  cells/ml. Before each cell experiment was performed, 10  $\mu\text{l}$  of suspension was diluted in a 1.5 ml sucrose solution with a concentration of 0.2M.

### III. RESULTS AND DISCUSSION

#### A. Correction factor of Stokes' law

Since the diameters of these two kinds of cancer cells are restricted to the range of 8–15  $\mu\text{m}$ , as shown in Fig. 5(a), standard polystyrene beads with diameters ranging from 5 to 25  $\mu\text{m}$  were tested for their sedimentation motion in DI water, 0.1M sucrose solution, and 0.2M sucrose solution for calibrating the correction factor associated with Stokes' law. However, we

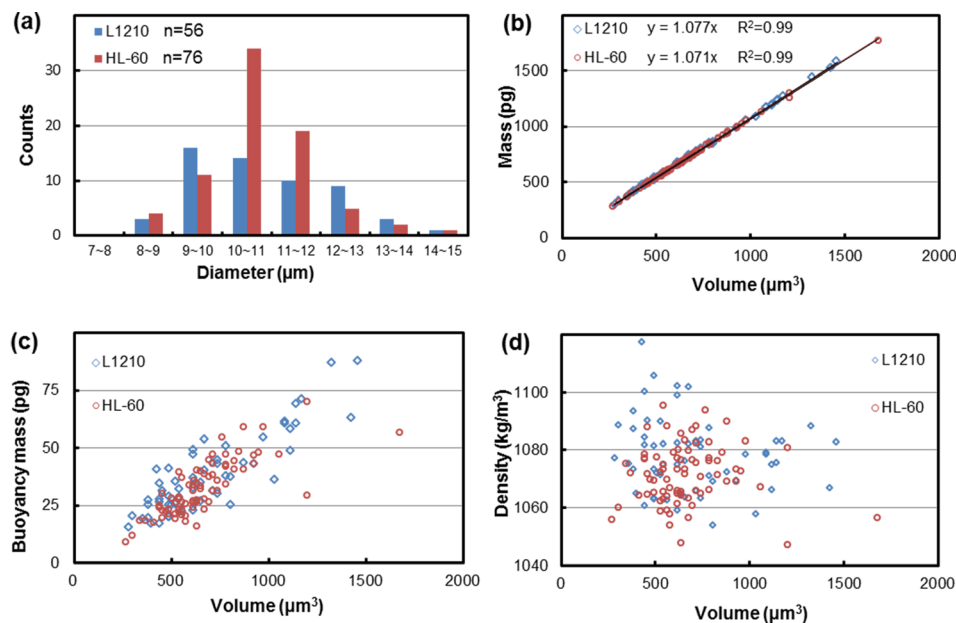


FIG. 5. Comparing results from the two kinds of cancer cells (L1210 and HL-60): (a) diameter distribution; (b) variation in mass with volume; (c) variation of buoyancy mass (buoyancy density multiplied by cell volume) with volume; and (d) variation in density with volume. The data shown are from 56 individual L1210 cells and 76 HL-60 cells.

found that the calculated velocity values were somewhat different from expectations of classical theory. According to Taylor's classical lubrication theory, the correction factor,  $K$ , for Stokes' force should comply with Eq. (3). According to this theory, the falling velocity of a particle should be as quickly as that indicated by the line with blue dots in Fig. 6(a), whereas our experiment data showed that the beads' falling velocity was actually much slower as indicated by the line with red dots. Our previously work<sup>17</sup> had found that a constant, " $a = 2.0$ ," should be used, as discussed previously in Eq. (4), based on hundreds of experimental data using different standard beads sedimenting in DI water. Experimental data from five kinds of beads in three types of solutions have shown that as long as the cells are spherical and have diameters around 5–25  $\mu\text{m}$ , setting the correction factor, " $a$ ," at 2.0 will give a reasonable estimate of the mass and density of the cell under observation. This difference from the Taylor's model may have arisen from the falling distance assumption, i.e.,  $h \ll r$  in Eq. (3), is not valid in our experiments. Furthermore, Taylor's model is based on the experimental data obtained from millimeter scale spheres, whereas our experimental data are based on micron-scale spheres.

In fact, the calibration process was used not only to calculate the correction factor but also to assess the accuracy of the method. As shown in Fig. 6(a), experiments were performed on three different individual beads of the same type. The results showed that the three data sets are very consistent, which indicated that the proposed method is stable and accurate enough to determine the motions of particles. Fig. 7 shows all of the results from the calibration experiments and analyses of the relationship between the correction factor, " $a$ ," and the diameters of the spheres, solution viscosities, and the densities of the different spheres and solutions. Note that the correction factor, " $a$ ," remains constant while these parameters vary. Based on these experimental results, it can be concluded that the proposed method is acceptable for measuring cell masses provided the Brownian motion effects on individual cells can be neglected, i.e., when the cell diameter remains in the range of 5–25  $\mu\text{m}$ . This diameter range covers most kinds of cells. In fact, it seems reasonable to extend the method to analyze even larger cells and particles. And, according to Piazza's work,<sup>25</sup> the transition between the Brownian and non-Brownian regimes takes place in the quite narrow range  $0.5 \mu\text{m} < r < 1.5 \mu\text{m}$ , which means that when the diameter of the microspheres is bigger than 3  $\mu\text{m}$  then its sedimentation process will not be affected by the Brownian motion.

As the motion of the sedimenting particles are assumed to have a linear relationship between the velocity  $U$  and the fluidic drag force without the influence of the rotation of the spheres, we had to make sure experimentally that the micro spheres did not rotate significantly. In our experiments (from testing more than 100 cells), we have not found any cell rotation during the "free falling" sedimentation process. We should however note that cell rotation have been observed when a DEP force is present in an OEK chip;<sup>15</sup> but, in this work, such a force was present for just about 1 s, so no cell rotation was observed.

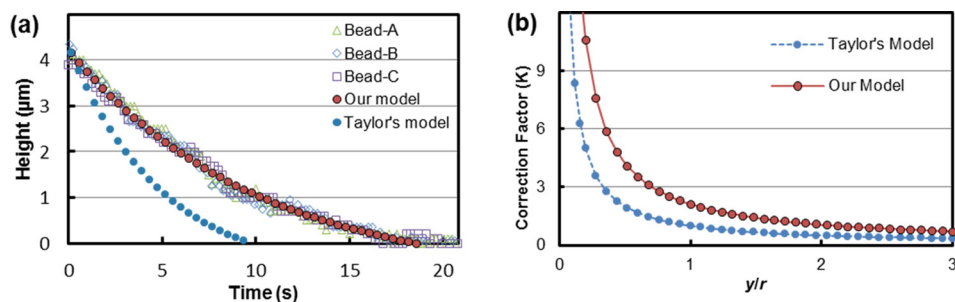


FIG. 6. (a) Time-lapsed height variation plots of microbeads with diameter of 10  $\mu\text{m}$ . The figure shows experimental data for three different polystyrene spheres of the same size. The red solid dotted lines are the results of curve fitting to Eq. (4), calculated by setting  $a = 2.0$ . The blue dotted lines are the curves calculated from Taylor's classical lubrication theory marked as the Taylor's model. (b) Comparison between estimates from Taylor's model and our model.



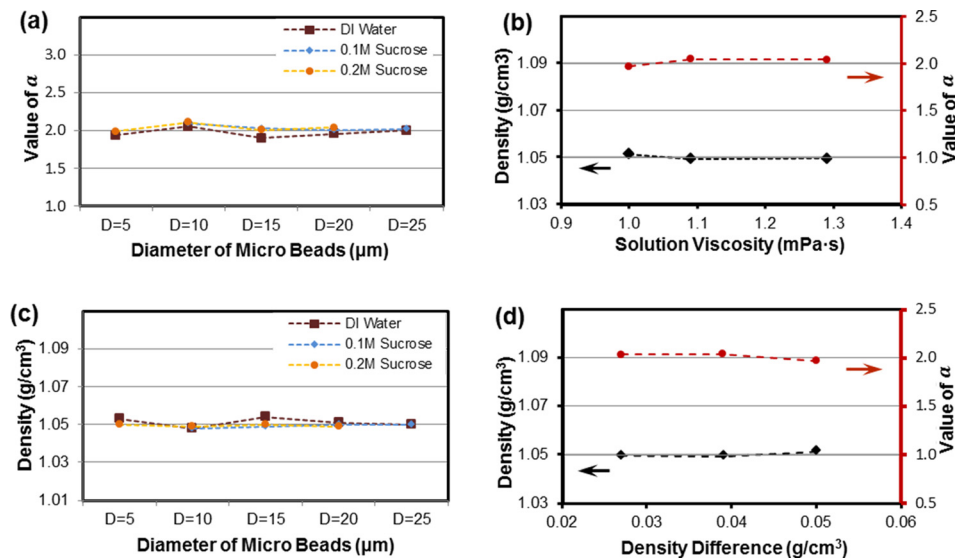


FIG. 7. (a) Five kinds of microbeads (diameters varying from 5 to 25  $\mu\text{m}$ ) were tested in three different kinds of solutions (DI water, 0.1M and 0.2M sucrose solution). If the densities of the microbeads ( $1.05 \text{ g}/\text{cm}^3$ ) are known, the value of  $a$  in our correction factor model are calculated as in the upper plot (a). On the other hand, if  $a$  is set 2.0, the calculated densities of the microbeads are as shown in (c). Based on our experimental results, the calculated densities and the values of  $a$  do not vary with (b) the solution viscosity and (d) the density difference between the particle and the solution significantly.

## B. Density and mass values of single cells

Using the method described above, we measured the density and the mass values of 56 individual L1210 cells. Results show that the densities of L1210 cells varied between 1.05 and 1.12  $\text{g}/\text{ml}$ , while the mass values were in the range of 350–1600 pg. This result conforms broadly with those obtained by the SMR method, as presented in Table I. This finding demonstrates that our method is practical for measuring the density and the mass of a single cell.

The advantage of the SMR method is that, because the technique utilizes the direct relationship between the shift in the resonance frequency of a cantilever beam and the cell mass, there is no need to consider effects attributable to cell shapes. However, the experimental device and equipment required for applying the SMR method are more complicated than those associated with the method proposed in this paper. The new method is based on the assumption that the cell under observation is nearly spherical in shape; only then can the equations proposed above be used to determine the cell mass/density. Therefore, the equations would need to be corrected for cells of shapes that far from being spherical—most likely by including a shape correction factor in the equations. However, fortunately, most of the cells in the suspension medium used by us were close to being spherical, so the proposed technique is applicable generally for the purpose of determining the mass/density values of many types of cells.

Although HL-60 cells have been widely researched for many years, we could not find any relevant data on the density and mass of single HL-60 cell in the literature, therefore, we could not check our experimental data as of now.

TABLE I. Comparison between the L1210 cell mass/density values measured by the OEK-based method proposed in this paper and those by the SMR method.

Method	Reference	Density ( $\text{g}/\text{ml}$ )	Volume ( $\mu\text{m}^3$ )	Mass (pg)
SMR <sup>a</sup>	Bryan <sup>5</sup> (2014) and Grover <sup>1</sup> (2011)	1.05–1.11	350–1300	400–1400
OEK	This report	1.05–1.12	300–1500	350–1600

<sup>a</sup>The results of SMR are combined from these two references listed.

#### IV. CONCLUSION

We have presented a single leukemia cell density and mass determination method using an OEK platform, which is based on a combination of computer vision, microparticle manipulation, and sedimentation theory principles in this paper. The falling trajectory and velocity of individual cells or micro beads could be tracked and calculated utilizing micro-vision processing technique. We have also presented an original method capable of evaluating the hydrodynamic interactions of an individual micron-sized sphere as it falls toward an infinite solid plane in an aqueous solution. Based on the experimental results, the correction factor of the Stokes' force has been validated by adding a constant parameter describing how the viscous force varies with falling distance when a micron-sized spherical particle falls perpendicular to an infinite plane in an aqueous solution of sucrose. Finally, we tested two kinds of mammalian leukemia cells and reported the results for the cellular mass and density values of 132 individual cancer cells. The results on L1210 are consistent with those from SMR tests, which demonstrate that our method is a practical, rapid, accurate, and multiplicative measurement technology for single cancer cell mass and density.

#### ACKNOWLEDGMENTS

The authors gratefully acknowledge support from the Hong Kong Research Grants Council (Project Nos. CityU 118513 and CityU 11215614), the Chinese Academy of Sciences—Croucher Funding Scheme for Joint Laboratories (Project No. 9500011), and the Nanshan Core Technology Breakthrough Project KC2013JSJS0003A.

- <sup>1</sup>W. H. Grover, A. K. Bryan, M. Diez-Silva, S. Suresh, J. M. Higgins, and S. R. Manalis, *Proc. Natl. Acad. Sci. U.S.A.* **108**, 10992 (2011).
- <sup>2</sup>H.-W. Wu, C.-C. Lin, and G.-B. Lee, *Biomicrofluidics* **5**, 13401 (2011).
- <sup>3</sup>T. P. Burg, M. Godin, S. M. Knudsen, W. Shen, G. Carlson, J. S. Foster, K. Babcock, and S. R. Manalis, *Nature* **446**, 1066 (2007).
- <sup>4</sup>M. Godin, F. F. Delgado, S. Son, W. H. Grover, A. K. Bryan, A. Tzur, P. Jorgensen, K. Payer, A. D. Grossman, M. W. Kirschner, and S. R. Manalis, *Nat. Methods* **7**, 387 (2010).
- <sup>5</sup>A. K. Bryan, V. C. Hecht, W. Shen, K. Payer, W. H. Grover, and S. R. Manalis, *Lab Chip* **14**, 569 (2014).
- <sup>6</sup>K. Park, L. J. Millet, N. Kim, H. Li, X. Jin, G. Popescu, N. R. Aluru, K. J. Hsia, and R. Bashir, *Proc. Natl. Acad. Sci. U.S.A.* **107**, 20691 (2010).
- <sup>7</sup>K. Park, J. Jang, D. Irimia, J. Sturgis, J. Lee, J. P. Robinson, M. Toner, and R. Bashir, *Lab Chip* **8**, 1034 (2008).
- <sup>8</sup>E. A. Corbin, L. J. Millet, K. R. Keller, W. P. King, and R. Bashir, *Anal. Chem.* **86**, 4864 (2014).
- <sup>9</sup>M. Meselson, F. Stahl, and J. Vinograd, *Proc. Natl. Acad. Sci. U.S.A.* **43**, 581 (1957).
- <sup>10</sup>P. Y. Chiou, A. T. Ohta, and M. C. Wu, *Nature* **436**, 370 (2005).
- <sup>11</sup>W. Liang, L. Liu, S. H.-S. Lai, Y. Wang, G.-B. Lee, and W. J. Li, *Opt. Mater. Express* **4**, 2368 (2014).
- <sup>12</sup>Y. Zhao, W. Liang, G. Zhang, J. D. Mai, L. Liu, G.-B. Lee, and W. J. Li, *Appl. Phys. Lett.* **103**, 183702 (2013).
- <sup>13</sup>W. Liang, Y. Zhao, L. Liu, Y. Wang, Z. Dong, W. J. Li, G.-B. Lee, X. Xiao, and W. Zhang, *PLoS One* **9**, e90827 (2014).
- <sup>14</sup>M. Ouyang, W. Ki Cheung, W. Liang, J. D. Mai, W. Keung Liu, and W. Jung Li, *Biomicrofluidics* **7**, 054112 (2013).
- <sup>15</sup>L.-H. Chau, W. Liang, F. W. K. Cheung, W. K. Liu, W. J. Li, S.-C. Chen, and G.-B. Lee, *PLoS One* **8**, e51577 (2013).
- <sup>16</sup>N. Liu, W. Liang, L. Liu, Y. Wang, J. Mai, G. Lee, and W. Li, *Lab Chip* **14**, 1367 (2014).
- <sup>17</sup>Y. Zhao, H. S. S. Lai, G. Zhang, G.-B. Lee, and W. J. Li, *Lab Chip* **14**, 4426 (2014).
- <sup>18</sup>Z. Adamczyk, M. Adamczyk, and T. G. M. van de Ven, *J. Colloid Interface Sci.* **96**, 204 (1983).
- <sup>19</sup>A. Ambari, B. Gauthier-Manuel, and E. Guyon, *J. Fluid Mech.* **149**, 235 (1984).
- <sup>20</sup>B. U. Felderhof, *J. Chem. Phys.* **122**, 214905 (2005).
- <sup>21</sup>D. Baigl, *Lab Chip* **12**, 3637 (2012).
- <sup>22</sup>A. Maude, *Br. J. Appl. Phys.* **12**, 293 (1961).
- <sup>23</sup>H. Brenner, *Chem. Eng. Sci.* **16**, 242 (1961).
- <sup>24</sup>N. Lecoq and F. Feuillebois, *Phys. Fluids A* **5**, 3 (1993).
- <sup>25</sup>R. Piazza, *Rep. Prog. Phys.* **77**, 056602 (2014).